Interaction of Dynamic Strain Aging and Transformation of Retained Austenite to Martensite

R. Bartels, D. Löhe and E. Macherauch, Institut für Werkstoffkunde I, Universität Karlsruhe, FRG

Depending on the carbon content and the type and the amount of alloying elements, hardened steels consist of martensite, retained austenite and carbides. Although a large number of investigations has been performed in recent years, several aspects of the influence of retained austenite on the mechanical behaviour of hardened steels are still controversially discussed. This is mainly a consequence of the fact that state and deformation properties of hardened steels are strongly influenced by many parameters. The idea to produce (for a given steel) hardened states with different amounts of retained austenite which are microstructurally equal cannot be realized physically. Nevertheless, investigations of high carbon steels where the amount of retained austenite can simply be varied by changing the austenitizing temperature, seem to be very useful. Of particular interest are quenched states with relatively large volume fractions of retained austenite. In alloyed steels, the martensite start temperature M_s can be shifted below room temperature if austenitization is performed at sufficiently high temperatures. After quenching to room temperature, the microstructure of such steels may solely consist of metastable austenite and carbide. This paper deals with the tensile deformation behaviour of a quenched and low tempered tool steel with 88 vol.-% retained austenite and 12 vol.-% carbide in the temperature range $-120\ ^{o}C \leq T \leq 150\ ^{o}C$.

Experimental details

The chemical composition of the material under investigation (German grade X 210 Cr 12, DIN 1.2080) was 2.08 C , 0.23 Si, 0.4 Mn, 0.009 S, 12.7 Cr, 0.07 Mo, 0.06 Ni (all numbers in weight-%). Cylindrically shaped tensile specimens (gauge length 25 mm, gauge diameter 5 mm) were machined, then carefully polished mechanically and afterwards heat-treated in a microprocessor-controlled vacuum furnace (heating rate 10 °C/min, austenitization 40 min at 1120 °C, quenching in oil of 30 °C). Subsequently, all specimens were tempered 2 hours at 180 °C in oil and then cooled down to room temperature. The microstructure resulting from this treatment consists of an austenitic matrix with about 12 vol.-% carbides and is shown in Fig. 1. The carbides are distributed in the interior and at the boundaries of the austenite. No martensite could be detected metallographically. Also X-ray standard procedures were applied to determine the volume contents of martensite, carbides and retained austenite quantitatively [1]. The X-ray measurements of the heat-treated specimens agreed quite well with the metallographic observations. Using a dilatometer the martensite start temperature of the specimens was determined as $M_s = -10\ ^{o}C$ in agreement with extrapolated X-ray measurements.

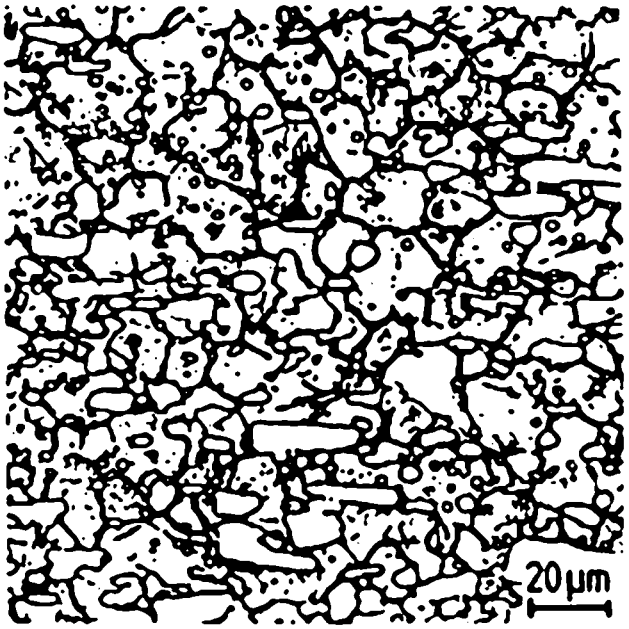

Fig. 1: Microstructure of the material state investigated.

Tensile tests were carried out in a universal testing machine equipped with a temperature chamber for $-120\ ^{o}C \leq T \leq 150\ ^{o}C$. The standard strain rate was $4.7 \cdot 10^{-4}\ s^{-1}$. In order to analyse dynamic strain aging effects, the strain rate was varied between $2.2 \cdot 10^{-6}$ and $3.3 \cdot 10^{-2}\ s^{-1}$. Integral and local strain measurements were performed with inductive extensometers and strain gauges, respectively. Changes of the inductivity of the tensile specimens during deformation were measured with an induction coil system working with a carrier frequency of 5 kHz.

Experimental results

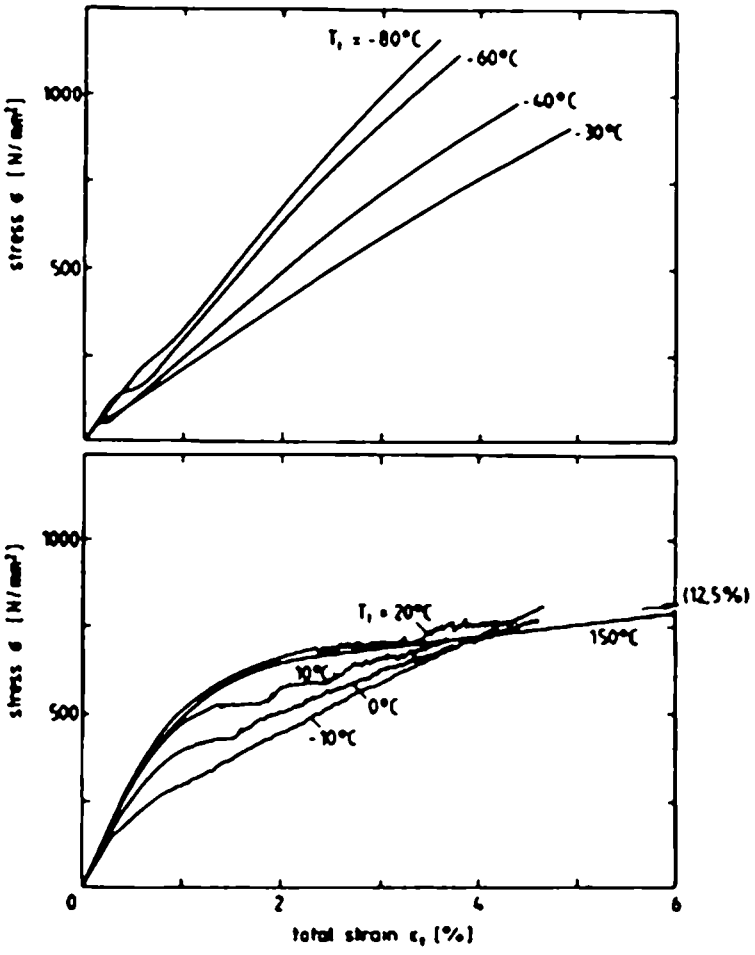

Fig. 2: Stress-strain curves at test-temperatures between -80 °C and -30 °C (upper part) and between -10 °C and 150 °C (lower part)

Fig. 2 shows typical stress-total strain curves of the material state under investigation for the temperature range $-80\ ^{o}C \leq T \leq 150\ ^{o}C$. In the upper part of the figure the results received at and below -30 °C are sketched. The lower part of the figure displays those obtained at -10 °C and at higher temperatures. Below -10 °C all stress-strain curves exhibit at very small stresses a region of "easy gliding" and have a smooth course. The stress-strain curves measured between -10 °C and +20 °C show jerky and serrated flow, respectively. At 150 °C again a smooth work-hardening curve is observed with an elongation to fracture of 12.5 %. The elongations to fracture at the other temperatures are markedly smaller, having a relative minimum around 10 °C and decreasing continuously at temperatures lower than -30 °C. The flow stresses of the regions of easy gliding increase with decreasing temperature. However, their magnitudes are smaller than those at comparable strains at temperatures above -30 °C. Also the work-hardening rates following the regions of easy gliding at larger strains are rather high and increase with decreasing test temperature.

In Fig. 3 changes of inductivity ΔI of the specimens at various test temperatures are drawn as a function of total tensile strain. These changes of inductivity are due to alterations of the permeability which in turn are a consequence of deformation-induced formation of martensite in the measured volume of the specimen. In the interval $-30\ ^{o}C \leq T \leq +20\ ^{o}C$, an increase in the slope of the curves with decreasing test temperature is observed. At -30 °C and -40 °C nearly identical curves are obtained. A further reduction of the test temperature to -60 °C and -80 °C results in a pronounced decrease of the slope of the $\Delta I, \varepsilon_t$-curves. It can be seen from a comparison of Figs. 2

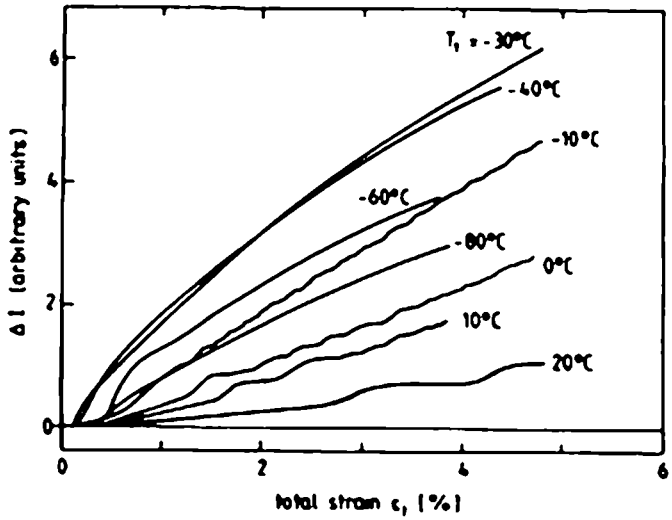

Fig. 3: Increase of inductivity ΔI during tensile straining at various test temperatures.

and 3 that unstable flow at the stress-total strain curves correspond to an unsteady run of the inductivity changes vs. strain. However, there is no direct proportionality between both quantities. At 20 °C, e. g., pronounced serrations occur in the stress-strain curve, whereas the observed changes of inductivity are rather weak. On the other hand, at -10 °C, where jerky flow is faint, a remarkable increase in inductivity appears. Furthermore, the regions of easy gliding in the stress-total strain curves between -30 °C and -80 °C correspond to strong increases of inductivity.

Fig. 4. summarizes X-ray determined amounts ΔRA of retained austenite transformed to martensite due to straining the specimens to fracture at different temperatures. Besides of the data from the gauge length, also results from the fracture surfaces of the specimens are shown. The quantities ΔRA were determined with respect to the values measured at the specimen ends, where without any influence of deformation only thermally induced martensitic transformations were possible. It becomes obvious that in the gauge length of all specimens strained in the temperature range between +20 °C and -120 °C austenite is transformed to martensite the amount of which is the largest at -40 °C. At higher and lower test temperatures smaller amounts of transformation are observed. Above +20 °C no evidence for a deformation-induced formation of martensite is found within the gauge length of the specimen. However, as can be seen from the upper curve in Fig. 4, in the temperature range from -120 °C to +20 °C markedly higher amounts of transformation occur at the fracture surfaces than within the gauge length. Furthermore, relative intense martensite formations happen there up to 150 °C. Fig. 5 supports that the changes of inductivity at elongation to fracture in Fig. 3 and the transformed amounts of retained austenite in Fig. 4 show an equivalent temperature dependence.

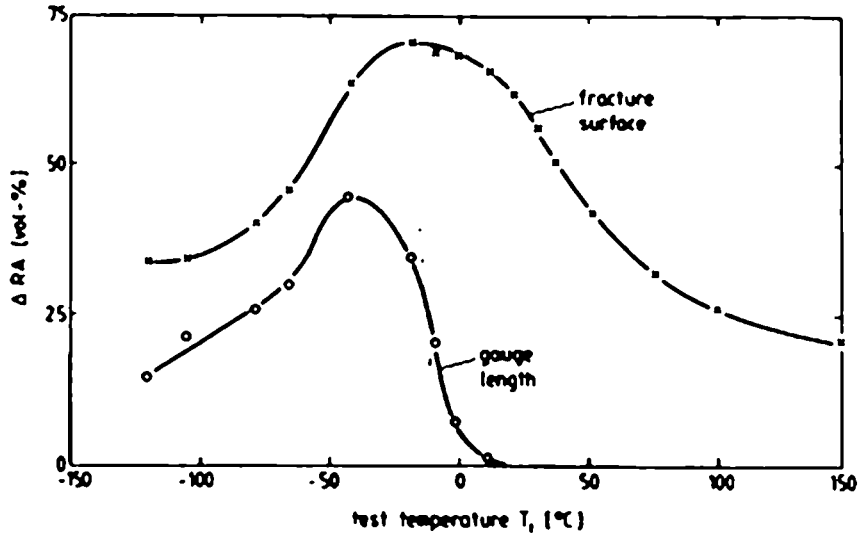

Fig. 4: Volume fraction of austenite ΔRA transformed to martensite during tensile straining in the gauge length and near the fracture surface as a function of test temperature.

Discussion

The most remarkable experimental findings in the temperature range investigated are the regions of easy-gliding and unstable flow at the workhardening curves. The phenomenon of easy-gliding is thought to be a consequence of transformation induced plasticity. However, below the martensite start temperature M_S = -10 °C the stress of starting easy gliding increases with decreasing temperature. Obviously, the retained austenite still existing at lower temperatures than M_S is mechanically stabilized by thermally induced martensite formation during cooling down to these temperatures.

Since above M_S the driving force for austenite transformation decreases with increasing temperature, the amounts of deformation induced transformations are also expected to decrease. This is confirmed by the results in Fig. 3. Nevertheless between -10 °C and +20 °C serrated and jerky flow does occur, respectively. These phenomena are often attributed solely to the formation of martensite from metastable austenite [2-8]. On the other hand, these events of unstable flow show features of dynamic strain aging. The critical strains at the onset of the serrations increase with increasing deformation temperature, which is well-known for type II dynamic strain aging effects in other alloys [9].

Furthermore, a comparison of the results from Fig. 2 and Fig. 3 shows no direct and simple correlation between stress jumps and measured changes of inductivity. In most cases several stress jumps seem to cause a single step-like increase of inductivity. Thus, it appeared helpful to registrate with higher resolution simultaneously the changes of stress and inductivity during tensile deformation. Results of a corresponding experiment performed at 20 °C are shown in Fig. 6. The crosshead displacement is proportional to the total strain. When exceeding the yield stress, a slight increase of inductivity is observed, which may be attributed to the formation of martensite in regions where slip bands interact [12]. However, when the first stress drop appears, the continuous increase of inductivity stops. Afterwards inductivity begins to grow in a stepwise manner, whereby at first the ΔI-steps increase with increasing total strain and then decrease again until ΔI becomes nearly constant. Thereafter, the whole process is repeated again. Later on the σ, ε_t- and the $\Delta I, \varepsilon_t$-curves become more and more irregular.

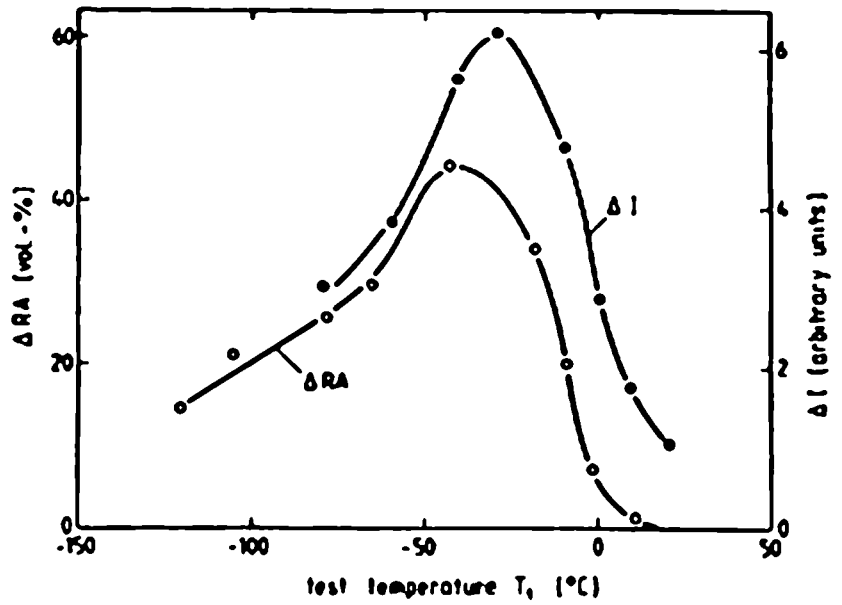

Fig. 5: Volume fraction of austenite ΔRA transformed to martensite in the gauge length and increase of inductivity ΔI during tensile straining to fracture as a function of test temperature.

These observations can be explained with the insert in Fig. 6, which visualize the measuring conditions at the deformation states 1, 2 and 3. Passing the loading stress over the yield strength R_{eS}, general yield induces martensite formations in the whole volume producing an integral increase of ΔI. If the first stress jumps at state 1 are correlated with a localized

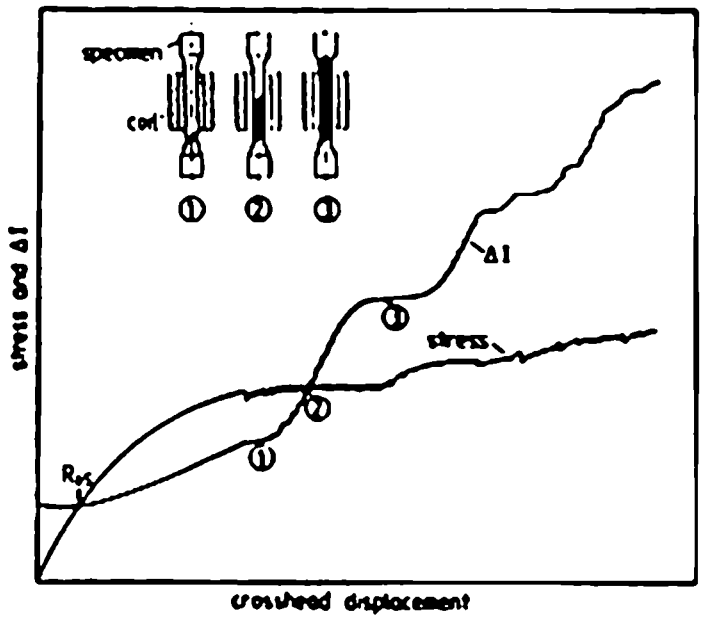

Fig. 6: Stress and change of inductivity during tensile straining and the movement of a deformation front through an inductive coil (insert) at room temperature.

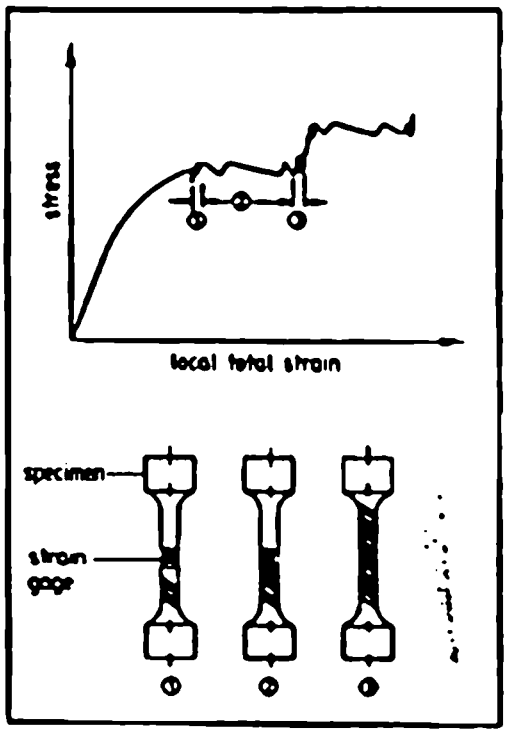

Fig. 7: Stress-local strain curve (upper part) and the spreading of local deformation bands (schematic sketch, lower part) at room temperature.

creation of deformation bands at one or both grip section(s) of the specimen, the corresponding martensite formations are unable to contribute to changes of inductivity, since they are produced outside the coil of the measuring system. If, however, deformation bands develop in those material regions which are surrounded by the coil, step-like increases of inductivity are expected in agreement with the experimental observations. Highest steps should be created in state 2 where the martensite formation occurs entirely within the coil volume. Finally, the measured jumps of inductivity become smaller and disappear, when the deformation front leaves the end of the coil (state 3). If this idea is right, a strain gauge applied to the middle part of a tensile specimen as illustrated in the lower part of Fig. 7 should measure only elastic strain changes as long as the deformation bands (sketched by short thick lines) develop outside the strain gauge (states 1 and 3). But elastic-plastic strain changes should appear if deformation bands develop in the area where the strain gauge is attached (state 2). The upper part of Fig. 7 shows the result of a corresponding experiment performed at 20 °C. In states 1 and 3 local deformations take place outside the strain gauge. Consequently, only elastic stress drops are registrated. In state 2, strain jumps occur within the active length of the strain gauge and are resolved in the local workhardening curve. The measured signals depend on the amount of the local deformations relative to the active length of the strain gauge. They increase with decreasing gauge length, until the width of the deformation bands of approximately 0.2 to 1 mm is reached. If the developing deformation bands approach the opposite grip section of the specimen, the whole process is repeated once more in a very similar way.

A further evidence that unstable flow is caused by the development of local deformation bands can be found by microscopic investigations of polished specimens. In agreement with the observations and conclusions presented above first deformation bands develop

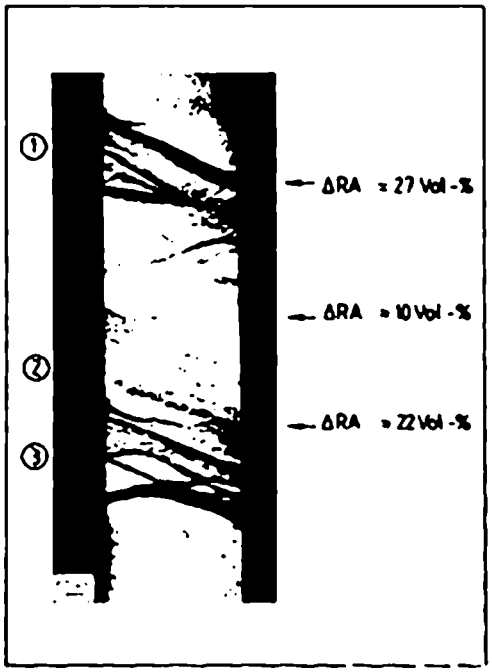

Fig. 8: Volume fraction of austenite transformed to martensite during tensile straining inside and outside of localized deformation bands.

in the transition area between the grips and the gauge length of the tensile specimen. Afterwards deformation bands one after another appear along the gauge length. If the total gauge length of the specimen is filled with deformation bands, the same procedure is repeated again. As an example, in Fig. 8, the micrograph of the surface of a flat specimen deformed at 20 °C until three stress drops occurred is shown. Within and outside the deformation bands also X-ray determinations of the locally transformed retained austenite ΔRA were carried out. The measured values are indicated. The deformation bands reveal changes of 22 and 29 vol.-%, which are markedly higher than the 10 vol.-% observed in between. After etching such a deformed specimen, also the microstructures within and outside the deformation bands display characteristic differences. This can be seen from Fig. 9. In the picture at the bottom, which belongs to a deformation band, most of the large carbides are cracked in contrast to an area outside a deformation band shown in the picture at the top. Additionally, much more martensite has been formed inside than outside the deformation band.

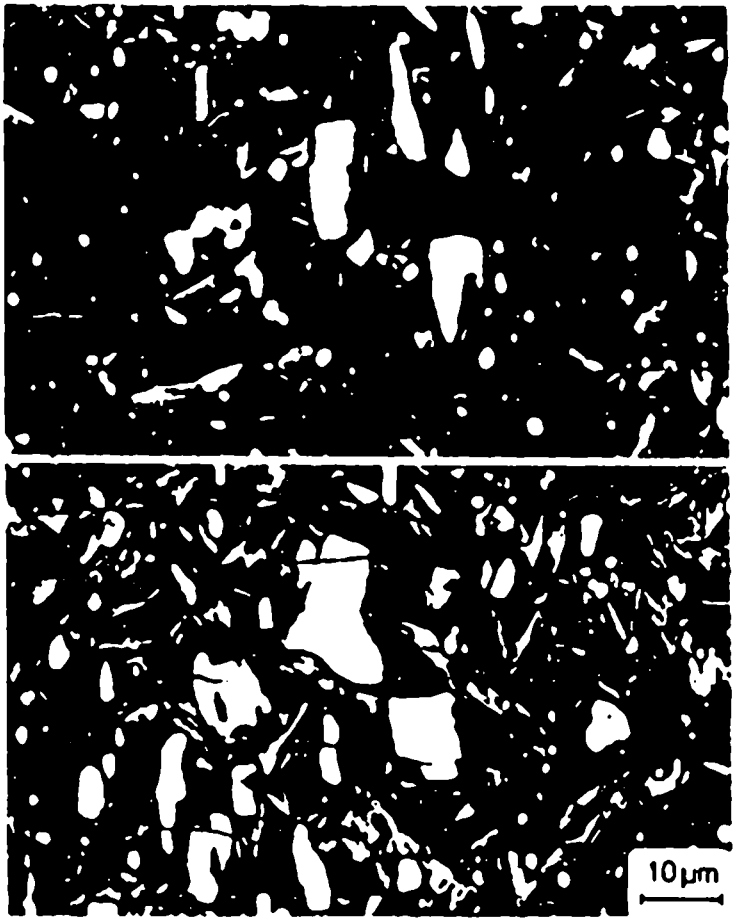

Fig. 9: Microstructure after fracture at room temperature inside (lower part) and outside (upper part) of a localized deformation band.

All experimental observations presented above suggest that the unstable flow of the material state investigated is a combined effect of dynamic strain aging and localized austenite transformation. However, unstable flow was registrated at test temperatures as low as -10 °C. An austenitic Hadfield steel with a high content of solved carbon also showed dynamic strain aging down to -20 °C [10]. In contrast, normalized plain carbon steels with low carbon contents reveal dynamic strain aging effects only at deformation temperatures higher than 60 °C [11]. Thus, it is believed that in the material state under investigation the austenite, which is a strongly supersaturated solid solution of carbon and chromium in iron, is able to reveal dynamic strain aging effects at relative low temperatures. As mentioned already, the critical strains ε_c at the onset of unstable flow increase with increasing test temperature. If this phenomenon is thermally activated, ε_c should decrease with increasing strain rate at a fixed deformation temperature. Fig. 10 shows the results of corresponding experiments at 20 °C which reveal the

expected behaviour. Furthermore, the flow stresses decrease with increasing strain rate, which is also expected during the occurrence of dynamic strain aging. If one assumes that the relationship

$$\dot{\varepsilon} = \alpha\, \varepsilon_c^r \exp\left[-\frac{E_a}{kT}\right]$$

(α, r constants, E_a apparent activation energy, k Boltzman constant, T absolute temperature) holds for the onset ε_c of unstable flow [9,11], plots of log ε_c vs. log $\dot{\varepsilon}$ and log ε_c vs. 1/kT should be represented by straight lines. Fig. 11 proves this to be true for the material state under investigation. The slopes of the curves are negative. From this fact and from the serrated appearance of the workhardening curves, one has to conclude that the so-called "type II dynamic strain aging" [11] occurs in the ranges of strain rate and temperature covered by Fig. 11. According to the equation given above, the slopes of the log ε_c vs. log $\dot{\varepsilon}$ and log ε_c vs. 1/kT-plots should be equal to 1/r and E_a/r, respectively. It comes out that r = -11 and E_a/r = -0.4 eV, resulting in an apparent activation energy E_a = r·E_a/r = 4.4 eV. Obviously, this value cannot be attributed to a simple thermally activated process. Thus, further research has to be done to clarify the observed interaction of dynamic strain aging and phase transformation in the material investigated.

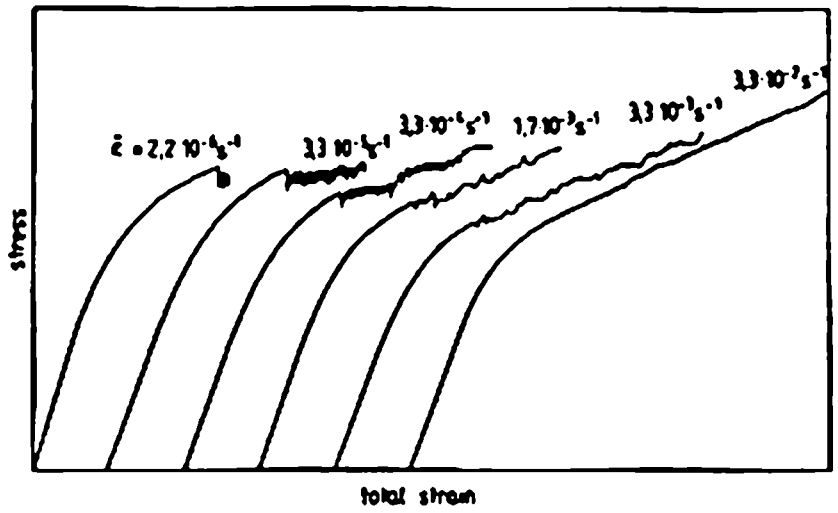

Fig. 10: Influence of strain rate on stress strain curves at room temperature.

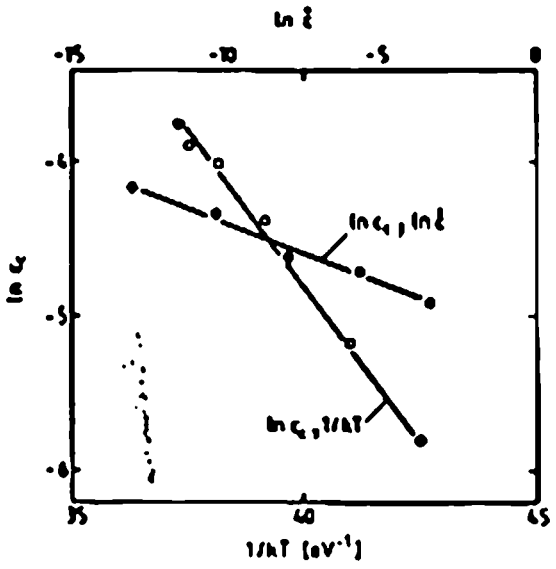

Fig. 11: Influence of strain rate and test temperature on the critical strain ε_c at the onset of unstable flow.

The support of these investigations by the Deutsche Forschungsgemeinschaft is gratefully acknowledged.

References

[1] R. Bartels: Dr.-Ing. Diss., Universität Karlsruhe (1987).
[2] H. Berns: Härterei-Tech. Mitt. 29 (1974), 236.
[3] F. Abrassart: Thèse, Université de Nancy I, (1972).
[4] G. F. Bolling, R. H. Richman: Acta Met. 14 (1970) 673.
[5] J. A. Hall, V. F. Zackay, E. R. Parker: Trans. ASM 62 (1969) 965.
[6] N. A. Kozleva, D. V. Lebedev: Mat. Scl. Heat Treatm. (1965) 825.
[7] W. Krüppers: Thyssen Edelst. Tech. Ber. 10 (1984) 44.
[8] G. R. Chanani, V. F. Zackay, E. R. Parker: Met. Trans 2 (1971) 133.
[9] D. Löhe, O. Vöhringer, E. Macherauch: Proc. 6th Int. Conf. Strength of Metals and Alloys (ICSMA 6), vol.1. Pergamon Press, Oxford (1982) 199.
[10] Y. N. Dastur, W. C. Leslie: Met. Trans 12A (1981) 749.
[11] K. Hültebräucker, O. Vöhringer, E. Macherauch: Proc. 5th Int. Conf. Strength of Metals and Alloys (ICSMA 5), vol. 2. Pergamon Press, Oxford (1979) 1037.
[12] H. Dietrich, DEW-Tech. Ber. 12 (1972) 199.